Analysis of the decay $K_L \to \pi^0\gamma\gamma$ and expectations for the decays $K_L \to \pi^0 e^+ e^-$ and $K_L \to \pi^0 \mu^+ \mu^-$

P. Heiliger
III. Physikalisches Institut A, Rheinisch-Westfälische Technische Hochschule Aachen, D-5100 Aachen, Germany

L. M. Sehgal
Institut für Theoretische Physik E, Rheinisch-Westfälische Technische Hochschule Aachen, D-5100 Aachen, Germany
(Received 16 November 1992)

A two-component model of the decay $K_L \to \pi^0\gamma\gamma$, in which the amplitude is the sum of a pion-loop contribution and a vector-meson-mediated term, is compared with data from the NA31 and E731 experiments. An estimate is obtained for the parameter G characterizing the strength of the vector-meson component. The amplitude of $K_L \to \pi^0\gamma\gamma$, determined in this way, is used to calculate the *CP*-conserving amplitude of the decays $K_L \to \pi^0 e^+ e^-$ and $K_L \to \pi^0 \mu^+ \mu^-$, without neglect of lepton masses. This complex amplitude (containing both absorptive and dispersive parts) is allowed to interfere with the *CP*-violating amplitude expected from the short-distance interaction $s\bar{d} \to l^+ l^-$ and from the *CP* impurity of the K_L wave function. Results are obtained for the branching ratios of $K_L \to \pi^0 l^+ l^-$ and for the *CP*-violating $l^+ l^-$ asymmetry in the Dalitz plot.

PACS number(s): 13.20.Eb, 11.30.Er, 12.15.Ji, 13.40.Hq

I. INTRODUCTION

The recent appearance of experimental data on the decay $K_L \to \pi^0\gamma\gamma$ [1–3] offers an opportunity to assess various theoretical proposals concerning the rate and spectrum of this reaction and its implications for the decay $K_L \to \pi^0 l^+ l^-$. A convenient framework for discussing the theoretical issues is a two-component picture of $K_L \to \pi^0\gamma\gamma$ described in Ref. [4]. In this picture the amplitude of the decay is the sum of two terms which correspond to two physically distinct mechanisms that have been envisaged for this reaction (Fig. 1). The first mechanism is the transition $K_L \to \pi^+\pi^-\pi^0$ followed by the annihilation of the $\pi^+\pi^-$ pair into two photons. This amplitude (called the pion-loop contribution) was calculated many years ago [5] and remains a good approximation to the meson-loop amplitude calculated in present-day discussions based on chiral perturbation theory [6]. The second mechanism involves the presence of a ρ or ω meson in the intermediate state, the final state being reached through the action of $\rho\pi\gamma$ and $\omega\pi\gamma$ vertices. This second piece of the amplitude [called the vector-meson-dominance (VMD) component] is uncertain, and its strength was parametrized in Ref. [4] by an unknown constant G. It was shown that the interference of the two components affects the branching ratio of the process and, simultaneously, the shape of the $\gamma\gamma$ mass distribution in a way that depends on the constructive or destructive nature of this interference. The recent data on $K_L \to \pi^0\gamma\gamma$ are of interest in that they allow a test of the two-component picture and provide an empirical estimate of the VMD contribution, which, in turn, has a bearing on the *CP*-conserving contribution to the decays $K_L \to \pi^0 l^+ l^-$.

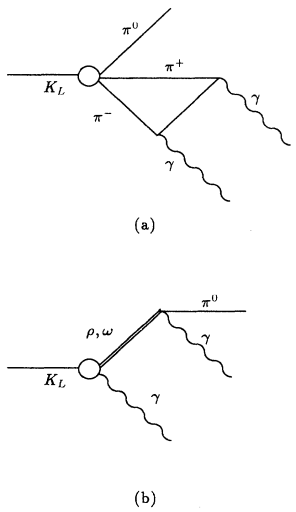

FIG. 1. (a) Pion-loop and (b) VMD contributions to $K_L \to \pi^0\gamma\gamma$.

In Sec. II we recapitulate the structure of the $K_L \to \pi^0\gamma\gamma$ amplitude in the two-component model and calculate the branching ratio as a function of the VMD parameter G. The shape of the $\gamma\gamma$ spectrum is presented for representative values of this parameter. Theoretical estimates of G are summarized, and a specific determination, based on the decays $K_L \to \gamma\gamma$ and $K_L \to \pi^+\pi^-\gamma$, is given in the Appendix. Finally, the theoretical framework is compared with the data of Refs. [1–3], and conclusions are drawn about the size of the VMD component.

In Secs. III and IV we consider the *CP*-conserving contribution to the decays $K_L \to \pi^0 e^+ e^-$ and $K_L \to \pi^0 \mu^+ \mu^-$, which is connected to the process $K_L \to \pi^0\gamma\gamma$. The two independent form factors charac-

terizing the amplitude for $K_L \to \pi^0 l^+ l^-$ are calculated, without neglecting the mass of the lepton. The resulting amplitude contains both absorptive and dispersive parts. In particular, the absorptive part of the $K_L \to \pi^0 \mu^+ \mu^-$ amplitude is shown to imply a lower limit of about 0.3×10^{-11} for the branching ratio of this decay.

In Sec. V we consider the *CP*-violating contribution to the decays $K_L \to \pi^0 l^+ l^-$ expected from short-distance effects and from the *CP* impurity of the K_L wave function. The latter contribution depends on the amplitude of $K_S \to \pi^0 l^+ l^-$, which is the major uncertain element in the analysis. The *CP*-violating amplitude is superposed on the *CP*-conserving part calculated in Secs. III and IV. Results are obtained for the branching ratio of $K_L \to \pi^0 l^+ l^-$, the $l^+ l^-$ mass spectrum, and the *CP*-violating $l^+ l^-$ asymmetry in the Dalitz plot.

II. DECAY $K_L \to \pi^0\gamma\gamma$

A. Two-component model

On grounds of *CP* and gauge invariance, the amplitude of $K_L \to \pi^0\gamma\gamma$ can be written in terms of two independent invariant amplitudes A and B as follows [4,6], where the symbols are defined in Fig. 2:[1]

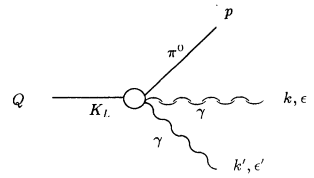

FIG. 2. Definition of momenta in $K_L \to \pi^0\gamma\gamma$.

$$\mathcal{M} = A(\epsilon\cdot k'\epsilon\cdot k - \epsilon\cdot\epsilon' k\cdot k') + B(\epsilon\cdot\epsilon' k\cdot Qk'\cdot Q + k\cdot k'\epsilon\cdot Q\epsilon'\cdot Q - \epsilon\cdot Q\epsilon'\cdot kk'\cdot Q - \epsilon\cdot kk\cdot Q\epsilon'\cdot Q)/k\cdot k' \ . \quad (1)$$

The amplitudes A and B are functions of the kinematical variables

$$s = (k+k')^2 \ , \quad \Delta = t - t' = (Q-k)^2 - (Q-k')^2 \ ,$$

which can be regarded as the coordinates of the Dalitz plot.

The pion-loop contribution [Fig. 1(a)] was calculated in Ref. [5]. It yields an amplitude of type A, with a dependence on the variable s alone[2] (μ = pion mass):

$$A_{\text{loop}} = \text{Re}\, A_{\text{loop}} + i\, \text{Im}\, A_{\text{loop}} \ , \quad (2a)$$

$$\text{Im}\, A_{\text{loop}} = 2\left[\frac{ge^2}{4\pi}\right]\frac{\mu^2}{s^2}\ln\frac{\sqrt{s}+(s-4\mu^2)^{1/2}}{\sqrt{s}-(s-4\mu^2)^{1/2}}\Theta(s-4\mu^2) \ , \quad (2b)$$

$$\text{Re}\, A_{\text{loop}} = \frac{1}{4\pi}\left[\frac{ge^2}{4\pi}\right]\frac{1}{s}\left\{\left[\frac{2\mu^2}{s}\left[\pi^2 - \ln^2\frac{\sqrt{s}+(s-4\mu^2)^{1/2}}{\sqrt{s}-(s-4\mu^2)^{1/2}}\right]-2\right]\Theta(s-4\mu^2) + \left[\frac{8\mu^2}{s}\left[\arctan\frac{1}{(4\mu^2/s-1)^{1/2}}\right]^2 - 2\right]\Theta(4\mu^2-s)\right\} . \quad (2c)$$

Here g is the coupling constant for $K_2 \to \pi^+\pi^-\pi^0$, derived from the central density of the Dalitz plot:

$$|g| = 0.84 \times 10^{-6} \ . \quad (3)$$

The VMD contribution [Fig. 1(b)] was initially calculated by Morozumi and Iwasaki [7] in a model in which the weak interaction was represented by $K_2 \to P$ vertices ($P = \pi, \eta, \eta'$), the final $\pi^0\gamma\gamma$ state being reached via $PV\gamma$ couplings ($V = \rho, \omega$). Quite generally, the VMD mechanism produces A- and B-type amplitudes, with the generic structure

$$A_{\text{VMD}} = -\frac{G}{2}\left[\frac{M_K^2+t}{t-M_V^2} + \frac{M_K^2+t'}{t'-M_V^2}\right] \ ,$$
$$B_{\text{VMD}} = -\frac{G}{2}\left[\frac{s}{t-M_V^2} + \frac{s}{t'-M_V^2}\right] \ . \quad (4a)$$

Here $G = G_\rho + G_\omega$, $G_{\rho,\omega}$ are the contributions of the ρ and ω intermediate states. (M_K is the K-meson mass and M_V the common mass of ρ and ω.) Specific models of the $K_2 V\gamma$ vertex yield specific values of the parameter G (which, in principle, can have a further dependence on t and t'). In Secs. III and IV, we shall also have occasion to use an approximate version of the form factors A_{VMD} and B_{VMD}, in which the t and t' dependence of the vector-meson propagator is neglected:

$$A_{\text{VMD}} \approx G_{\text{eff}}\frac{3M_K^2+\mu^2-s}{2M_V^2} \ ,$$
$$B_{\text{VMD}} \approx G_{\text{eff}}\frac{s}{M_V^2} \ . \quad (4b)$$

Taking both the pion-loop and VMD components into

[1] In Eq. (1) of Ref. [4], the overall sign of the A term should be changed.

[2] The expression for $\text{Re}\, A_{\text{loop}}$ was misprinted in Ref. [4]. The correct expression (which is the same as in Ref. [5]) was used in all the calculations reported in Ref. [4].

account, the full amplitude of $K_L \to \pi^0\gamma\gamma$ is characterized by the invariant form factors

$$A = A_{\text{loop}} + A_{\text{VMD}} , \quad B = B_{\text{VMD}} . \tag{5}$$

The differential decay rate in the variables s and Δ is [4]

$$\frac{d\Gamma}{ds\, d\Delta} = \frac{1}{2^{11}\pi^3 M_K^3} \left[|As - BM_K^2|^2 + \left[\frac{B}{s}\right]^2 (M_K^2\mu^2 - tt')^2 \right] , \tag{6}$$

with

$$tt' = \tfrac{1}{4}[(M_K^2 + \mu^2 - s)^2 - \Delta^2] .$$

The piece proportional to $|As - BM_K^2|^2$ corresponds to the $J=0$ state of the two photons, the remainder to $J=2$ [8]. The range of integration is

$$-\Delta_0(s) < \Delta < \Delta_0(s) , \quad 0 < s < (M_K - \mu)^2 , \tag{7}$$

with

$$\Delta_0(s) = [(M_K^2 + \mu^2 - s)^2 - 4M_K^2\mu^2]^{1/2} .$$

B. Branching ratio and two-photon mass spectrum

The model described above contains one unknown parameter G which determines simultaneously the branching ratio of $K_L \to \pi^0\gamma\gamma$ and the shape of the $\gamma\gamma$ mass spectrum. The results depend on the relative sign of the VMD parameter G and the pion-loop parameter g, and we will consider both constructive interference ($G/g > 0$) and destructive interference ($G/g < 0$). (These two cases will be referred to simply as $G > 0$ and $G < 0$.)

Figure 3 shows the basic features of the two-photon mass spectrum in four special situations: (a) pion-loop contribution only, (b) VMD contribution only with $|G| = 0.2\times10^{-7} M^{-2}$, (c) loop+VMD amplitude, $G = +0.2\times10^{-7} M_K^{-2}$ (constructive interference), and (d) loop+VMD amplitude, $G = -0.2\times10^{-7} M_K^{-2}$ (destructive interference). The branching ratios for these special cases are also indicated. (These distributions were also shown in Ref. [4], using the variable s instead of $m_{\gamma\gamma} = s^{1/2}$.)

In Fig. 4(a) we have plotted the branching ratio of the decay $K_L \to \pi^0\gamma\gamma$, separated into a high-mass ($m_{\gamma\gamma} > 280$ MeV) and low-mass ($m_{\gamma\gamma} < 280$ MeV) interval, for various values of G, both positive and negative. Such a plot (which was given in Ref. [9]) helps to illustrate how the total rate of this decay and its distribution in the $\gamma\gamma$ mass vary with the magnitude and sign of the VMD contribution. Figure 4(b) shows the same plot using the approximate version of the VMD amplitude given in Eq. (4b), the free parameter being G_{eff}. [From a comparison of Figs. 4(a) and 4(b), we note that a value $GM_K^2 = 0.2\times10^{-7}$ corresponds approximately to $G_{\text{eff}} M_K^2 = 0.25\times10^{-7}$.]

Finally, we indicate in Fig. 5 the distribution in the variable Δ (proportional to the difference of photon energies in the K^0 rest system) for four typical situations.

C. Comments on the loop contribution

As indicated in Fig. 3(a) the pion-loop model by itself yields a branching ratio 0.99×10^{-6}. About 60% of this

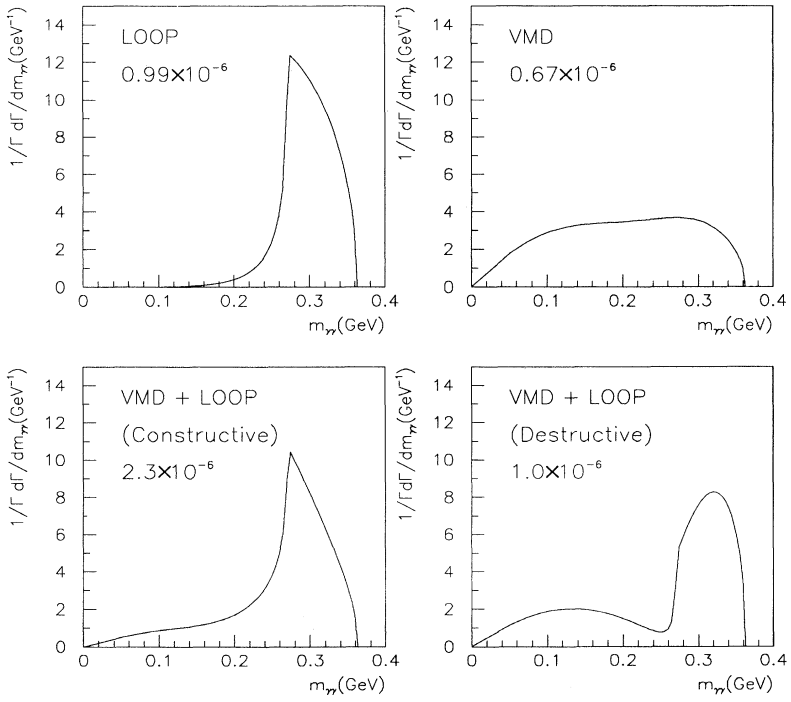

FIG. 3. Invariant mass spectra of $\gamma\gamma$ pair in the two-component model: four typical cases.

rate is absorptive, the rest dispersive. This estimate rests on the value g of the $K_L \to \pi^+\pi^-\pi^0$ coupling constant for which we have used the density at the center of the Dalitz plot, $s = s_0 = \frac{1}{3}M^2 + \mu^2$. It has been argued by Ko and Rosner [10] that inclusion of the slope of the Dalitz plot, extrapolated over the domain $0 < s < (M_K - \mu)^2$ appropriate to the decay $K_L \to \pi^0\gamma\gamma$, would yield a branching ratio 0.75×10^{-6}. In chiral perturbation theory [6], the s dependence of the $K_L \to \pi^+\pi^-\pi^0$ amplitude is automatically included, as is the contribution of the kaon loop (which, however, is only a 7% effect). The normalization of the chiral Lagrangian is fixed by the decay rate of $K_S \to \pi^+\pi^-$, leading to a branching ratio 0.68×10^{-6}, with a spectrum similar to that in Fig. 3(a). Our estimate of 0.99×10^{-6} is somewhat higher than that in these alternative approaches and thus more conservative from the point of view of interpreting an enhanced branching ratio in terms of a VMD effect.

D. Comments on the VMD contribution

The VMD parameter G has been estimated theoretically in several ways.

(i) The assumption that the parity-conserving nonleptonic weak interaction can be represented by the vertices $K_2 \to \pi$, $K_2 \to \eta$, and $K_2 \to \eta'$, and that these vertices are related to each other by the $\Delta I = \frac{1}{2}$ rule plus nonet symmetry, yields [7,11]

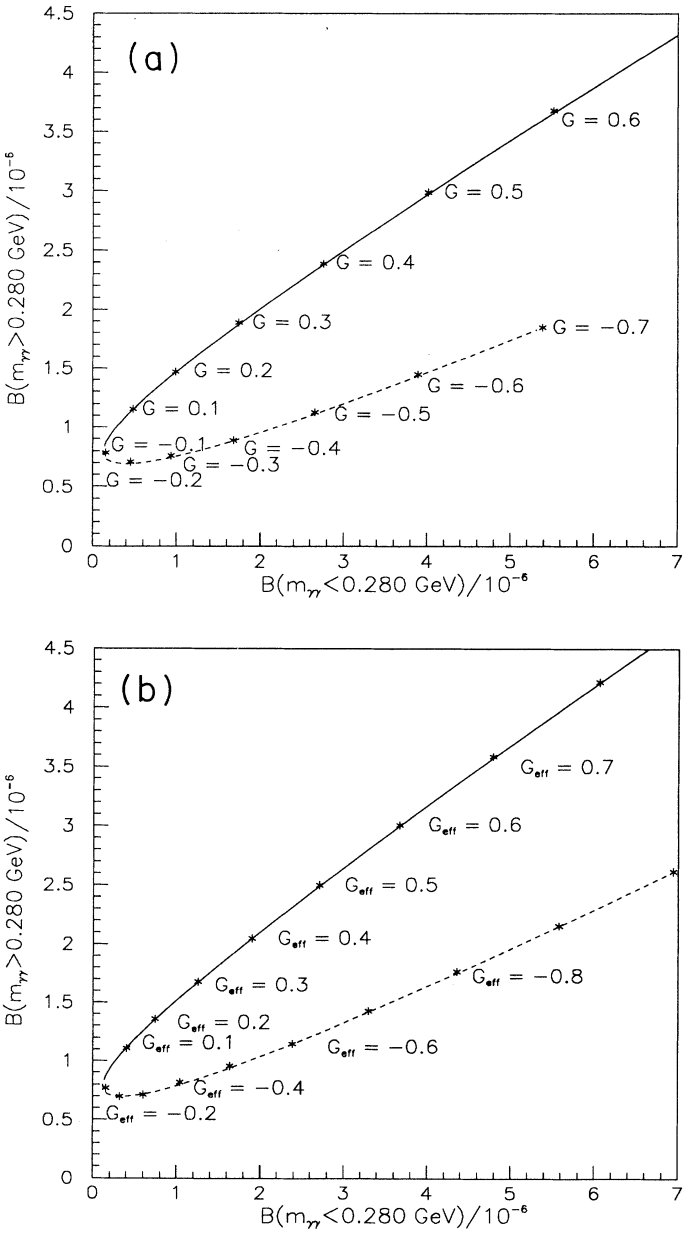

FIG. 4. Branching ratio of $K_L \to \pi^0\gamma\gamma$ in the mass intervals $m_{\gamma\gamma} > 280$ MeV and $m_{\gamma\gamma} < 280$ MeV, as a function of (a) the VMD parameter G and (b) the effective VMD parameter G_{eff}.

$$G_\rho M_K^2 = g_{\rho\pi\gamma}^2 \langle \pi^0|H_W|K_L\rangle \left[\frac{1}{1-r_\pi^2} + (\sqrt{3}\cos\Theta_P - \sqrt{6}\sin\Theta_P)\left[\frac{1}{\sqrt{3}}\cos\Theta_P + \frac{4}{\sqrt{6}}\sin\Theta_P\right]\frac{1}{1-r_\eta^2} \right.$$
$$\left. + (\sqrt{3}\sin\Theta_P + \sqrt{6}\cos\Theta_P)\left[\frac{1}{\sqrt{3}}\sin\Theta_P - \frac{4}{\sqrt{6}}\cos\Theta_P\right]\frac{1}{1-r_{\eta'}^2}\right], \quad (8)$$

$$G_\omega M_K^2 = g_{\omega\pi\gamma}^2 \langle \pi^0|H_W|K_L\rangle \left[\frac{1}{1-r_\pi^2} + \frac{1}{9}(\sqrt{3}\cos\Theta_P - \sqrt{6}\sin\Theta_P)\left[\frac{1}{\sqrt{3}}\cos\Theta_P + \frac{4}{\sqrt{6}}\sin\Theta_P\right]\frac{1}{1-r_\eta^2} \right.$$
$$\left. + \frac{1}{9}(\sqrt{3}\sin\Theta_P - \sqrt{6}\cos\Theta_P)\left[\frac{1}{\sqrt{3}}\sin\Theta_P - \frac{4}{\sqrt{6}}\cos\Theta_P\right]\frac{1}{1-r_{\eta'}^2}\right]. \quad (9)$$

Assuming the quark-model relation $g_{\rho\pi\gamma}^2 = \frac{1}{9} g_{\omega\pi\gamma}^2$, a pseudoscalar mixing angle $\Theta_P = -20°$, and a weak matrix element

$$\langle \pi^0|H_W|K_L\rangle = 2.9\times10^{-2}\ \text{MeV}^2 ,$$

as recommended by Truong [11], one obtains

$$G_\rho M_K^2 = -0.037\times10^{-7} , \quad G_\omega M_K^2 = -0.170\times10^{-7} , \quad (10)$$
$$|GM_K^2| \equiv |(G_\rho + G_\omega)M_K^2| = 0.207\times10^{-7} .$$

The uncertainty in the numerical values is related to the SU(3) assumption

$$\langle \eta_8|H_W|K^0\rangle / \langle \pi^0|H_W|K^0\rangle = (\tfrac{1}{3})^{1/2} ,$$

the nonet assumption

$$\langle \eta^0|H_W|K^0\rangle / \langle \pi^0|H_W|K^0\rangle = -2(\tfrac{2}{3})^{1/2} ,$$

and the value of Θ_P.

(ii) An alternative way of estimating G_ρ and G_ω, which avoids the explicit assumption of pseudoscalar-pole dominance, is to relate the VMD component of $K_2 \to \pi^0\gamma\gamma$ to the amplitudes for the decays $K_2 \to \pi^+\pi^-\gamma$ (direct emission) and $K_2 \to \gamma\gamma$, as illustrated in Fig. 6. All three amplitudes are expressed in terms of two phenomenological vertices $K_2\rho\gamma$ and $K_2\omega\gamma$ (see the Appendix for details). The resulting values for the parameters G_ρ and G_ω are (up to an overall sign)

$$G_\rho M_K^2 = +0.068\times10^{-7} , \quad G_\omega M_K^2 = -0.28\times10^{-7} , \quad (11)$$
$$|GM_K^2| \equiv |(G_\rho + G_\omega)M_K^2| = 0.21\times10^{-7} .$$

The above numerical result is obtained for an assumed value of $f_{\rho\pi\pi}^2/4\pi = 2.5$. Varying this from 2.2 to 2.9 changes $|GM_K^2|$ from 0.14×10^{-7} to 0.27×10^{-7}. Thus a generous error estimate is

$$|GM_K^2| = (0.2\pm0.1)\times10^{-7} . \quad (12)$$

Note that the central value is close to that in the pseudoscalar dominance approach. As in Eq. (10), the dominant contribution is that of the ω, but unlike (10), the ρ and ω contributions obtained in (11) have opposite signs.

(iii) Finally, we record the estimates obtained for the VMD parameter in the model of Ecker, Pich, and de Rafael (EPR) [12] in which vector mesons are introduced

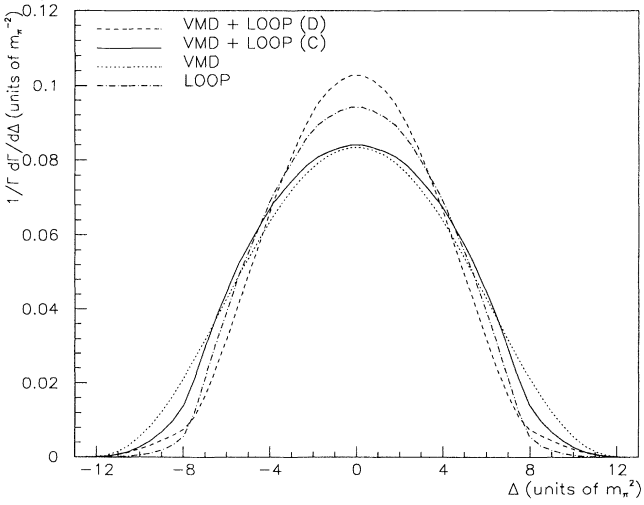

FIG. 5. Distribution of the decay $K_L \to \pi^0\gamma\gamma$ in the variable Δ in the two-component model with $|GM_K^2| = 0.2\times10^{-7}$. C (D) denote constructive (destructive) interference.

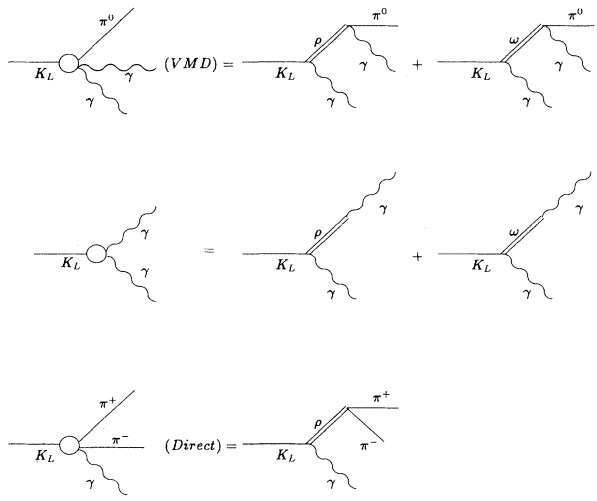

FIG. 6. Vector-meson contributions to $K_L \to \pi^0\gamma\gamma$, $K_L \to \gamma\gamma$ and direct emission part of $K_L \to \pi^+\pi^-\gamma$.

into a chirally symmetric Lagrangian through a "weak deformation" hypothesis. The analog of the form factor $B_{\rm VMD}$ obtained in this approach is

$$B_{\rm EPR}=2a_V\frac{G_8}{\pi}\frac{s}{M_K^2}\ , \tag{13}$$

where $G_8=9.1\times10^{-6}$ GeV^{-2} and a_V is estimated to be 0.32. Comparison with the generic form given in Eq. (3) shows that the t and t' dependence of the form factor B is neglected. Referring to the approximate form in Eq. (4b), the result (13) corresponds to

$$|G_{\rm eff}M_K^2|=0.08\times10^{-7}\ \ ({\rm EPR}) \tag{14}$$

(see Ref. [12]). This is a factor 2.5 smaller than the central value of the phenomenological estimate given in Eq. (12) above. (Still smaller values have been obtained in an approach based on the chiral quark model [13], which yields a form similar to (12), with $a_V=\frac{1}{9}$.)

E. Comparison with data on $K_2 \to \pi^0\gamma\gamma$

1. NA31 experiment

The NA31 experiment reported in 1990 [1] a branching ratio

$$B(K_L\to\pi^0\gamma\gamma, m_{\gamma\gamma}>280\ {\rm MeV})=(2.1\pm0.6)\times10^{-6}\ . \tag{15}$$

Comparison with the theoretical curve in Fig. 7(a) suggests (for constructive interference, $G>0$)

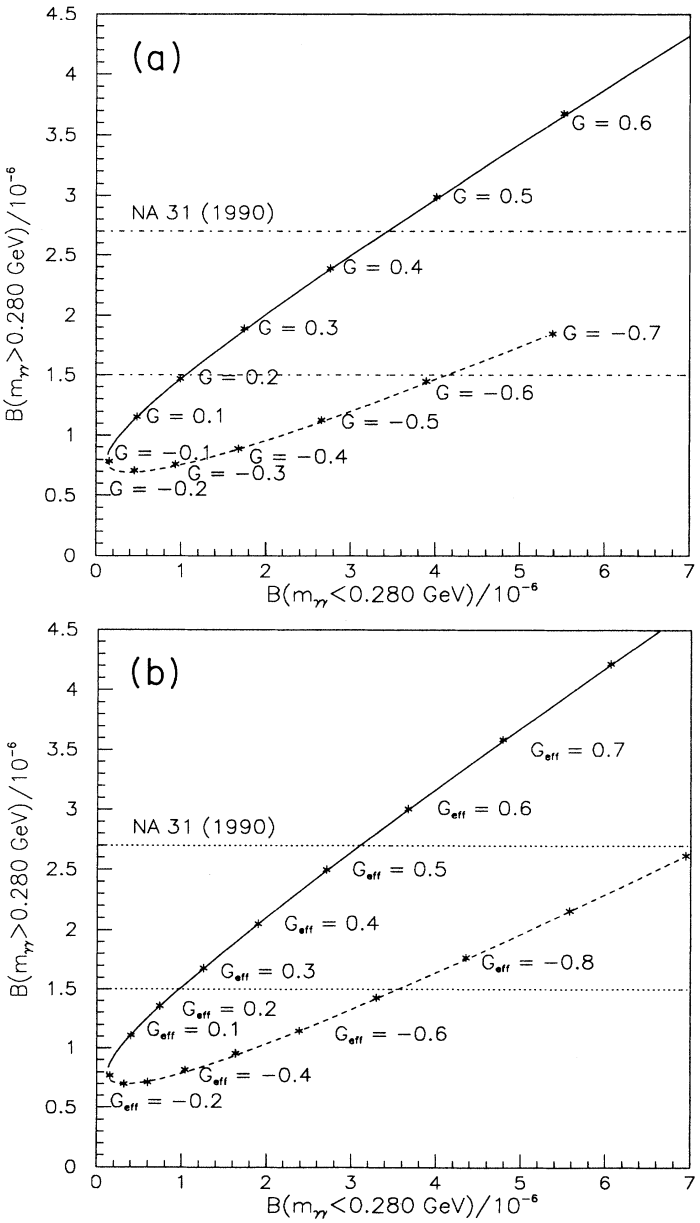

FIG. 7. Comparison of NA31 (1990) data [1] with two-component model. (a) Branching ratio as function of G, (b) branching ratio as function of $G_{\rm eff}$, (c) invariant mass distribution for $GM_K^2=0.3\times10^{-7}$, and (d) invariant mass distribution corrected for acceptance.

$$GM_K^2 = +(0.33 \pm 0.12) \times 10^{-7} \ . \quad (16)$$

For the value $GM_K^2 = 0.3 \times 10^{-7}$ of the VMD parameter, the theoretically expected 2γ spectrum is indicated in Fig. 7(c). A comparison with the experimental distribution is shown in Fig. 7(d), where we have multiplied the theoretical spectrum with the experimental acceptance given in Ref. [1].

More recently, the NA31 Collaboration has reported the results of a new analysis based on a larger sample of events [3]. The branching ratio of $K_L \to \pi^0\gamma\gamma$ (corrected for acceptance) is stated to be

$$B(K_L \to \pi^0\gamma\gamma) = (1.7 \pm 0.3) \times 10^{-6} \ , \quad (17)$$

somewhat lower than (but compatible with) the earlier result [Eq. (15)]. Comparison with the two-component model [Fig. 7(a)] yields a correspondingly lower value for the VMD parameter:

$$GM_K^2 = +(0.13 \pm 0.04) \times 10^{-7} \ . \quad (18)$$

The new data also provide a limit

$$\frac{\Gamma(m_{\gamma\gamma} < 240 \text{ MeV})}{\Gamma(\text{all } m_{\gamma\gamma})} < 0.09 \ (90\% \text{ C.L.}) \ . \quad (19)$$

The theoretical model gives for this ratio the value (0.13,0.18,0.22) for $GM_K^2 = (0.09, 0.13, 0.17) \times 10^{-7}$. Finally, the complete $\gamma\gamma$ distribution is compared with the theoretical model for $GM_K^2 = 0.13 \times 10^{-7}$ in Fig. 8, after allowance for the experimental acceptance. (The tenden-

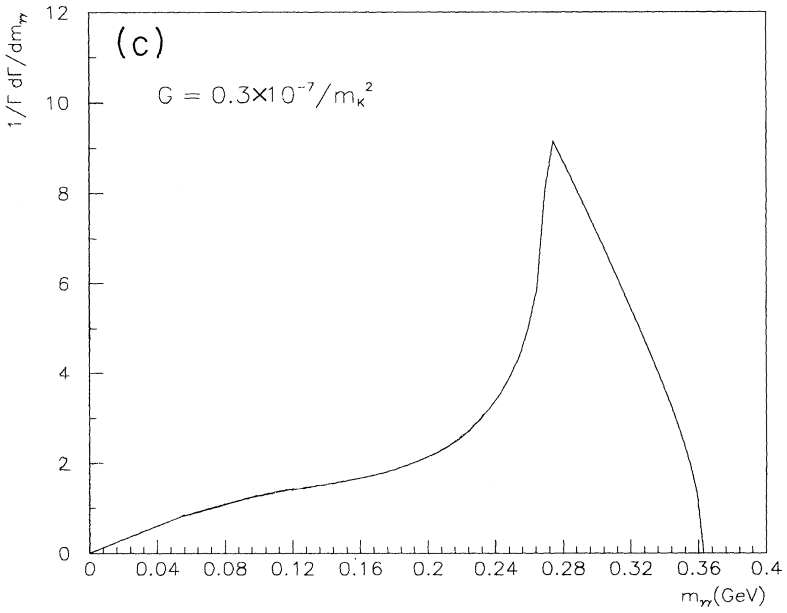

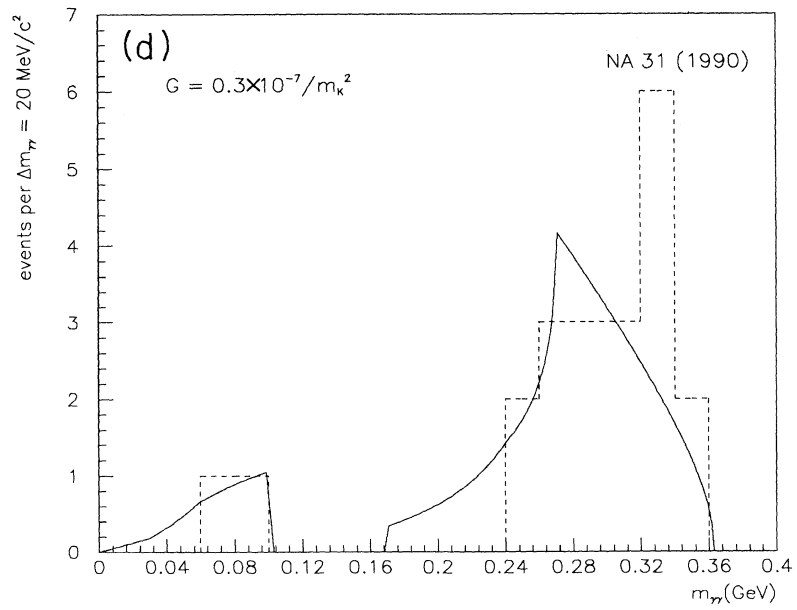

FIG. 7. (*Continued*).

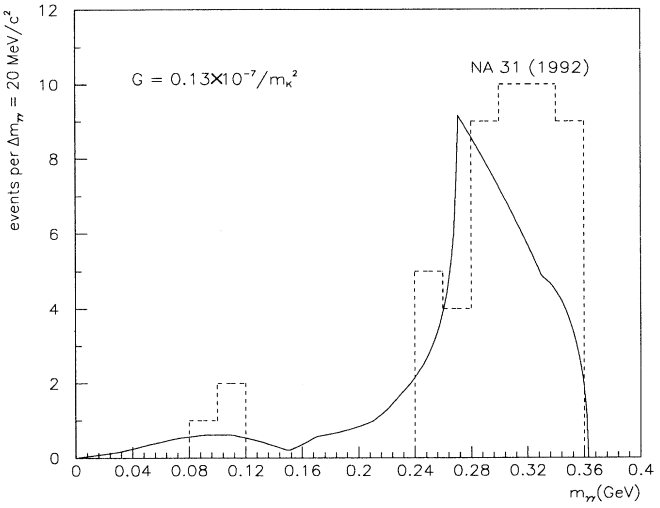

FIG. 8. Invariant mass distribution of NA31 (1992) data [3], compared with theoretical expectation for $GM_K^2 = 0.13 \times 10^{-7}$ (corrected for acceptance).

cy of the data to peak at somewhat higher values of $m_{\gamma\gamma}$ can be understood as an effect of the slope in the $K_L \to \pi^+\pi^-\pi^0$ matrix element [5,10,12].)

Finally, we show in Fig. 9(a) the distribution in the second Dalitz-plot variable Δ expected in the two-component model with $GM_K^2 = +0.13 \times 10^{-7}$ (constructive interference) and compare it with the distribution predicted by the loop model alone. The VMD admixture causes the distribution to fall less steeply with $|\Delta|$. The data of Ref. [3], reproduced in Fig. 9(b), also appear to be flatter than the prediction of chiral perturbation theory, in qualitative agreement with the above expectation. A quantitative comparison requires knowledge of the acceptance in the variable Δ.

From the various comparisons shown in Figs. 7–9, we conclude that the absolute branching ratio of $K_L \to \pi^0\gamma\gamma$, the $\gamma\gamma$ mass spectrum, and the distribution in Δ measured by NA31 can be brought into reasonable agreement with the two-component model, for a VMD parameter in the range $GM_K^2 = +(0.13 \pm 0.04) \times 10^{-7}$. This result is not at variance with the theoretical estimate given in Eq. (12). Our conclusion concerning the strength of the VMD component does not coincide with that reached in Ref. [3], which fits the shape of the $K_L \to \pi^0\gamma\gamma$ spectrum, without attempting to explain the absolute rate. [The result quoted in Ref. [3] is $-0.38 < a_V < 0.41$ (90% C.L.), which translates approximately into $|GM_K^2| < 0.10 \times 10^{-7}$ (90% C.L.).] It needs to be stressed that the prediction of the pion-loop model (and of chiral perturbation theory) is an absolute prediction, the normalization of which cannot be adjusted arbitrarily. A change in the prediction requires either higher-order corrections or a more complicated model for the $\pi\pi$ interaction. However, the absorptive part of the pion-loop amplitude (which accounts for two-thirds of the decay rate of this mechanism) is fixed by physical (mass-shell) amplitudes for $K_L \to \pi^+\pi^-\pi^0$ and $\pi^+\pi^- \to \gamma\gamma$, which are experimentally known and not negotiable. As a consequence, a fit in which the imaginary part of the pion-loop amplitude is multiplied by an overall factor can do violence to unitarity.

2. *E731 experiment*

The E731 experiment has measured the branching ratio of $K_L \to \pi^0\gamma\gamma$ for $m_{\gamma\gamma} > 280$ MeV [2],

$$B(K_L \to \pi^0\gamma\gamma, m_{\gamma\gamma} > 280 \text{ MeV}) = (1.86 \pm 0.60 \pm 0.60) \times 10^{-6}, \quad (20)$$

and gives an upper bound for $m_{\gamma\gamma} < 264$ MeV, using a phase-space distribution for $m_{\gamma\gamma}$:

$$B(K_L \to \pi^0\gamma\gamma, m_{\gamma\gamma} < 264 \text{ MeV}) < 5.1 \times 10^{-6}. \quad (21)$$

Comparison with the two-component (Fig. 10) gives

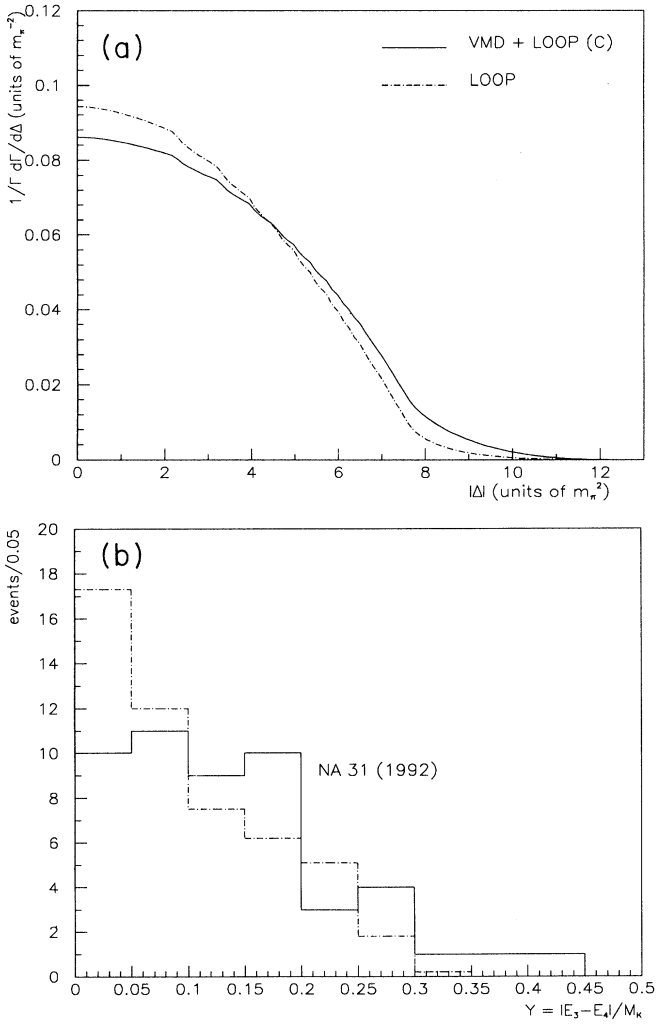

FIG. 9. Distribution in the variable Δ (or Y): (a) Model expectation (curve C corresponds to $GM_K^2 = 0.13 \times 10^{-7}$) and (b) NA31 data [3] (solid histogram) compared to chiral perturbation theory (dashed histogram).

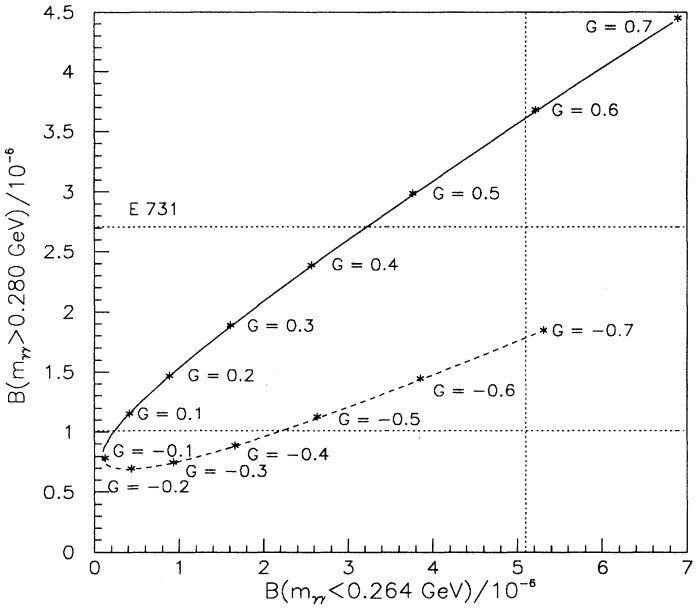

FIG. 10. Branching ratio of $K_L \to \pi^0\gamma\gamma$ measured in E731 [2] compared with two-component model.

$$GM_K^2 = +(0.25 \pm 0.20) \times 10^{-7} , \tag{22}$$

consistent with the estimates derived from the NA31 data.

In the remainder of this paper, we will assume that the amplitude of $K_L \to \pi^0\gamma\gamma$ is described by the two-component model, with a VMD parameter given by Eq. (18), and we will analyze the reactions $K_L \to \pi^0 e^+ e^-$, $K_L \to \pi^0 \mu^+ \mu^-$ on this basis. Results will be presented for the nominal value $GM_K^2 = 0.13 \times 10^{-7}$ (corresponding to $G_{\text{eff}} M_K^2 \approx 0.15 \times 10^{-7}$), which can be rescaled as necessary.

III. DECAY $K_L \to \pi^0 e^+ e^-$: CP-CONSERVING CONTRIBUTION

A. General structure of the amplitude

The decay $K_2 \to \pi^0 l^+ l^-$ can occur through a *CP*-violating one-photon intermediate state and a competing *CP*-conserving two-photon exchange amplitude [14] (see Fig. 11). An additional contribution arises from the short-distance interaction $s\bar{d} \to l^+ l^-$. The full amplitude of the decay

$$K_2(p) \to \pi^0(p') + l^-(k) + l^+(k')$$

can be written as

$$\begin{aligned} \mathcal{A}[K_2(p) \to \pi^0(p') l^-(k) l^+(k')] &= \bar{u}(k) \not{p} [F_V(s,\Delta) + F_A(s,\Delta)\gamma_5] v(k') \\ &\quad + \bar{u}(k) F_S(s,\Delta) v(k') , \end{aligned} \tag{23}$$

where we introduce

$$s = (k + k')^2 ,$$

$$t = (p - k)^2 , \quad t' = (p - k')^2 ,$$

$$\Delta = t - t' , \quad w = t + t' .$$

Chiral symmetry enforces that the form factor F_S be proportional to m_l and hence negligible for the decay $K_L \to \pi^0 e^+ e^-$. The form factors $F_{V,A}$ can be split into terms that are even or odd in Δ:

$$F_{V,A} = iF_{V,A}^{\text{even}}(s,\Delta) + F_{V,A}^{\text{odd}}(s,\Delta) . \tag{24}$$

For a *CP*-odd decaying state such as K_2, the even and

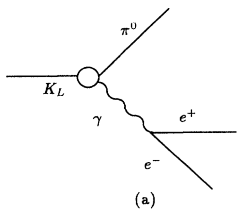

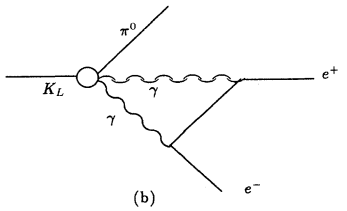

FIG. 11. Diagrams illustrating (a) one-photon and (b) two-photon contributions to $K_L \to \pi^0 e^+ e^-$.

odd parts correspond to a *CP*-violating and a *CP*-conserving amplitude. A factor i has been introduced since *CPT* invariance requires even and odd parts to be out of phase by 90°, provided there are no absorptive parts in the decay amplitude.

The two-photon intermediate state contributes to the form factor $F_S(s,\Delta)$, proportional to m_l, and to $F_V^{\rm odd}(s,\Delta)$. The latter contribution requires the existence of a B-type invariant in the $K_L \to \pi^0\gamma\gamma$ amplitude, which, in the two-component model discussed in Sec. II, is proportional to the VMD coupling G or $G_{\rm eff}$. The two-photon contributions to F_S and $F_V^{\rm odd}$ are complex; i.e., the *CP*-conserving amplitude has a large absorptive part. This leads to an interference term in the decay spectrum linear in Δ, resulting in an l^+l^- asymmetry in the Dalitz plot [14].

In terms of the form factors F_S, F_A, and F_V, the differential cross section for $K_L \to \pi^0 l^+ l^-$ is

$$\frac{d\Gamma}{ds\,d\Delta}=\frac{1}{256\pi^3 M_K^3}\left\{|F_V|^2\left[m_l^2\frac{\lambda}{s}+\frac{1}{4}(\lambda\beta^2-\Delta^2)\right]+|F_S|^2 s\beta^2 + |F_A|^2\left[m_l^2\left[\frac{\lambda}{s}+4M_K^2\right]+\frac{1}{4}(\lambda\beta^2-\Delta^2)\right]-2\,\mathrm{Re}(F_S F_V^*)m_l\Delta\right\}, \tag{25}$$

where

$$4m_l^2<s<(M_K-\mu)^2\ ,\quad -\Delta_0(s)<\Delta<+\Delta_0(s)\ ,$$

$$\Delta_0(s)=\beta[(M_K^2-\mu^2-s)^2-4\mu^2 s]^{1/2}\ ,$$

$$\beta=\left[1-\frac{4m_l^2}{s}\right]^{1/2}\ ,$$

$$\lambda=\lambda(M_K^2,\mu^2,s)=M_K^4+\mu^4+s^2-2sM_K^2-2s\mu^2-2M_K^2\mu^2\ .$$

B. Imaginary and real parts of F_1

We have calculated the two-photon contribution to the decay $K_2 \to \pi^0 l^+ l^-$ which is responsible for the form factor F_S as well as the term $F_V^{\rm odd}$. Applying the Cutkosky rule to the two-photon diagram (Fig. 11) and calculating the resulting integrals by the covariant method given in Ref. [15], we find, for the B-type matrix element of $K_2 \to \pi^0\gamma\gamma$ (which is the only relevant term for $K_2 \to \pi^0 e^+ e^-$),

$$\mathcal{A}(K_2 \to \pi^0 e^+ e^-)|_{2\gamma}=-\frac{\alpha}{16}\left[\frac{G_{\rm eff}}{M_V^2}\right]\bar{u}(k)F_1 \not{p} v(k')\ , \tag{26}$$

where

$$\mathrm{Im}F_1=-\frac{\Delta}{\beta^2}\left[\frac{2}{3}+\frac{2}{\beta^2}-\left[\frac{1}{\beta^2}-\beta^2\right]V\right] \overset{\beta\to 1}{\Longrightarrow} -\frac{8}{3}\Delta\ ,$$

with

$$V=\frac{1}{\beta}\ln\frac{1+\beta}{1-\beta}\ .$$

The limiting result for $\beta \to 1$ is in agreement with formula (28) of Ref. [16].[3] A plot of $\mathrm{Im}F_1/\Delta$ as a function of β is shown in Fig. 12.

In Eq. (26) and the corresponding calculation for $K_2 \to \pi^0\mu^+\mu^-$, we have used the approximate form of the invariants $A_{\rm VMD}$ and $B_{\rm VMD}$, given in Eq. (4b), for ease of analytic calculation.

To obtain the real part of F_1, we use a dispersion relation. The dispersion integral is logarithmically divergent, if we cut it off at a value $\Lambda^2 \sim m_\rho^2$, considering the vector-meson mass as a natural cutoff in the VMD model. We have

$$\mathrm{Re}F_1=\frac{1}{\pi}\int_{s_{\min}(\Delta)}^{\Lambda^2=m_\rho^2} ds'\frac{\mathrm{Im}F_1(s',\Delta)}{s'-s}\ , \tag{27}$$

where $s_{\min}(\Delta)$ is determined by the inequalities

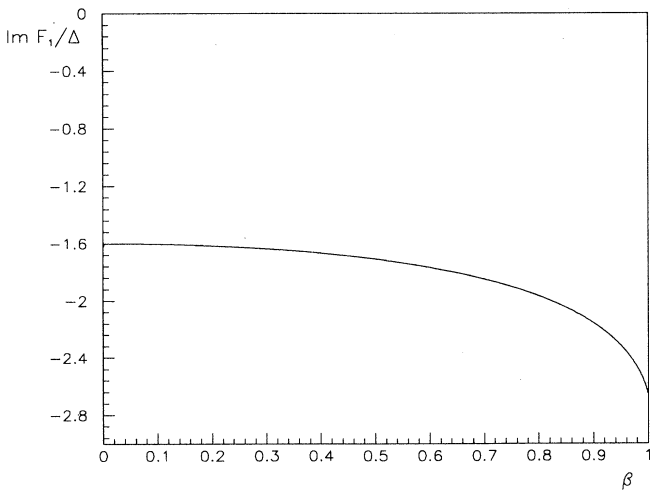

FIG. 12. Absorptive part of the form factor F_1 for $K_L \to \pi^0 l^+ l^-$.

[3]We thank G. Ecker for a communication explaining the origin of the correction factor $\frac{2}{3}$ to be applied to the results in the first two papers of Ref. [6], as pointed out by Ref. [16].

$$0 \le \Delta \le k_\pi \left[1-\frac{4m_l^2}{s}\right]^{1/2} 2M_K \ ,$$

$$0 \le k_\pi \le \frac{[(M_K+\mu)^2-4m_l^2]^{1/2}[(M_K-\mu)^2-4m_l^2]^{1/2}}{2M_K} \ , \tag{28}$$

where $k_\pi^2 = E_\pi^2 - \mu^2$ and $E_\pi = (M_K^2+\mu^2-s)/2M_K$.

C. Decay spectrum and decay rate

The resulting decay spectrum for the *CP*-conserving amplitude of $K_2 \to \pi^0 e^+ e^-$ is shown in Fig. 13 as a function of w/M_K^2, where w is related to the π^0 energy in the K_2 rest frame by $w = 2M_K E_\pi + 2m_l^2$. The spectrum is weighted toward large w, i.e., toward small invariant masses of the e^+e^- pair. Using Eqs. (26) and (27) we calculate

$$B(K_2 \to \pi^0 e^+ e^-)|_{2\gamma} = 4.6\times 10^{-12}\left[\frac{G_{\rm eff}}{0.25}\frac{M_K^2}{10^{-7}}\right]^2 (1+\rho) \ , \tag{29}$$

where

$$\rho = \frac{\Gamma_{\rm disp}}{\Gamma_{\rm abs}} \simeq 1.5 \ .$$

A previous estimate for the ratio of dispersive and absorptive parts, based on Cheng's analysis [17], was $\rho \sim 0.4$ [14]. Because of the cutoff dependence, these estimates have only qualitative significance, but they do indicate that the absorptive and dispersive parts of the two-photon amplitude for $K_L \to \pi^0 e^+ e^-$ are comparable.

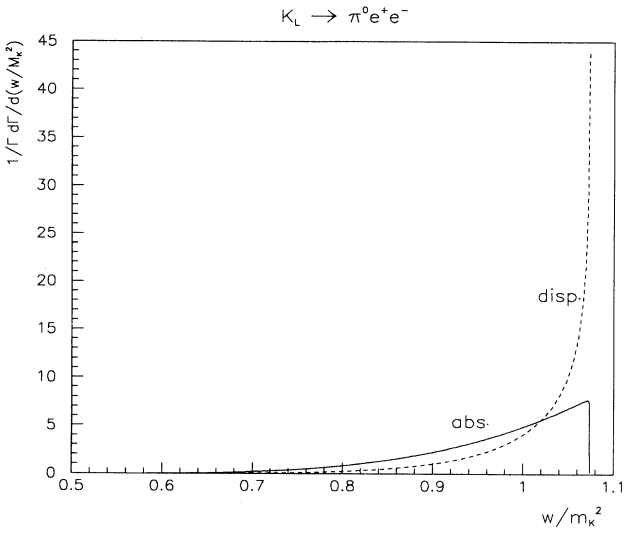

FIG. 13. Absorptive and dispersive contributions to e^+e^- spectra in $K_L \to \pi^0 e^+ e^-$ (*CP*-conserving part).

IV. DECAY $K_L \to \pi^0\mu^+\mu^-$: *CP*-CONSERVING CONTRIBUTION

A. Imaginary and real parts of F_1 and F_2

The decay $K_L \to \pi^0\mu^+\mu^-$ is of special interest because (i) one does not have to deal with the background from the process $K_2 \to \gamma\gamma e^+e^-$ with $m_{\gamma\gamma}^2 \simeq \mu^2$, which can simulate $K_L \to \pi^0 e^+ e^-$ [18], and (ii) contributions of form factors proportional to the lepton mass are no longer negligible and lead to an enhancement of the branching ratio of $K_L \to \pi^0\mu^+\mu^-$ over the naive phase-space expectation.

Analogous to Eq. (26), the *CP*-conserving amplitude for $K_L \to \pi^0\mu^+\mu^-$ can be written in the form

$$\mathcal{A}(K_2 \to \pi^0\mu^+\mu^-)|_{2\gamma} = -\frac{\alpha}{16}\bar{u}(k)\left[\frac{G_{\rm eff}}{M_V^2}F_1 \not{p} + F_2\right] v(k') \ , \tag{30}$$

where

$$F_2 = F_2^{(A)} + F_2^{(B)} + F_2^{\rm loop} \ .$$

The imaginary and real parts of F_1 are given in Sec. III B. The form factor F_2 is proportional to m_l and receives contributions from both the VMD and pion-loop amplitude in $K_L \to \pi^0\gamma\gamma$. For the B-type contribution $F_2^{(B)}$ of the $K_2 \to \pi^0\gamma\gamma$ intermediate state, we calculate

$$\begin{aligned}\mathrm{Im}F_2^{(B)} = \frac{2}{3}\frac{G_{\rm eff}}{M_V^2}\frac{m_l}{s\beta^6}\{ & -\Delta^2[30+\beta^2+\tfrac{3}{2}V(3\beta^2+\beta^4-10)] - (sM_K^2+\tfrac{1}{4}\lambda)[10(\beta^2+3)+3V(\beta^4-5)] \\ & + m_l^2 M_K^2[\tfrac{2}{3}(30+19\beta^2) - V(10+3\beta^2-3\beta^4)] \\ & + (s+M_K^2-\mu^2)^2[\tfrac{1}{2}(15+8\beta^2+7\beta^4) - \tfrac{3}{4}V(5+\beta^2+\beta^4+\beta^6)] \\ & - sM_K^2[\tfrac{1}{6}(30+25\beta^2-7\beta^4) - \tfrac{1}{4}V(10+5\beta^2-6\beta^4-9\beta^6)] \\ & + 3\beta^4[(M_K^2-\mu^2)^2 + s(s-2\mu^2)](V-2)\} \ .\end{aligned} \tag{31}$$

As may be checked, the expression for $\mathrm{Im}F_2^{(B)}$ is finite in the limit $\beta \to 0$. Furthermore, unlike $\mathrm{Im}F_1$, it has a dependence on s as well as Δ^2. For $\Delta = 0$ the function $\mathrm{Im}F_2^{(B)}/(G_{\rm eff} m_l M_K^2/M_V^2)$ is plotted in Fig. 14.

The form factor F_2 receives a further contribution from the A-type matrix elements for $K_2 \to \pi^0\gamma\gamma$. The corresponding absorptive part is given by

$$\mathrm{Im}F_2^{(A)} = 4A_{\mathrm{VMD}} m_l V = 4G_{\mathrm{eff}} \left[\frac{3M_K^2 + \mu^2 - s}{2M_V^2} \right] m_l V \ . \tag{32}$$

The function $\mathrm{Im}F_2^{(A)}/(G_{\mathrm{eff}} m_l M_K^2/M_V^2)$ is plotted in Fig. 14.

Again, we calculate the real parts of $F_2^{(A)}$ and $F_2^{(B)}$ by a dispersion relation of the form given in Eq. (27):

$$\mathrm{Re}F_2^{(A,B)} = \frac{1}{\pi} \int_{s_{\min}(\Delta)}^{\Lambda^2 = m_\rho^2} ds' \frac{\mathrm{Im}F_2^{(A,B)}(s', \Delta)}{s' - s} \ . \tag{33}$$

Finally, the "pion-loop" contribution to the decay $K_L \to \pi^0 \mu^+ \mu^-$ is illustrated in Fig. 15. This is a two-loop diagram which has an absorptive part from the 2γ intermediate state for $s > 4m_\mu^2$ and an additional absorptive contribution from the 2π intermediate state for $s > 4\mu^2$. The calculation of this two-loop amplitude is similar to that encountered for $K_1 \to \mu^+\mu^-$, which has been carried out by Ecker and Pich [19]. The real and imaginary parts of F_2^{loop} are given by

$$F_2^{\mathrm{loop}} = \frac{16}{\alpha_{\mathrm{em}}} \left[\frac{g_{K_2 \to \pi^+\pi^-\pi^0}}{g_{K_1 \to \pi^+\pi^-}} \right] \frac{\alpha_{\mathrm{em}}^2}{\pi^2} G_8 f_\pi m_l (1 - r_\pi^2)(I_{l,\mathrm{disp}} + iI_{l,\mathrm{abs}}) \ ,$$

$$I_{l,\mathrm{disp}} = \int_0^1 du \int_0^1 dv\, v \int_0^1 dy \left\{ \frac{2u + 2v - 1}{\beta_l} \left[1 - y + \ln \left| \frac{\alpha + \beta_l}{\alpha} \right| \left[1 - \frac{\alpha}{\beta_l}(1 - y) \right] \right] + \frac{u}{\alpha\gamma - \beta_l} \ln \left| \frac{\alpha + \beta_l}{\alpha(1 + \gamma)} \right| \right\} \ , \tag{34}$$

$$I_{l,\mathrm{abs}} = \pi \int_0^1 du \int_0^{1-u} dv\, v \int_0^1 dy \left\{ \Theta(-\alpha)\Theta(\alpha + \beta_l) \frac{2u + 2v - 1}{\beta_l^2} [\beta_l - \alpha(1 - y)] + \lim_{\epsilon \to 0} \frac{u(\alpha\gamma - \beta_l)}{(\alpha\gamma - \beta_l)^2 + \epsilon^2} [\Theta(-\alpha)\Theta(\alpha + \beta_l) - \Theta(r_\pi^2 - u(1 - u))] \right\} \ ,$$

where

$$\alpha = y[r_\pi^2 - v(1 - v)] \ ,$$

$$\beta_l = yv(1 - u - v) \left[1 - \frac{yu}{u + v} \right] + \frac{m_l^2}{s}(1 - y)^2(u + v)(1 - u - v) \geq 0 \ ,$$

$$\gamma = -1 + y \frac{u(1 - u) - r_\pi^2}{(u + v)(1 - u - v)} \ ,$$

$$r_\pi^2 = \frac{m_\pi^2}{s} \ .$$

G_8 is the octet coupling constant [19] with the numerical value $|G_8| \simeq 9 \times 10^{-6}$ GeV^{-2} determined from $\Gamma(K^0 \to 2\pi)$ using lowest-order chiral perturbation theory. $g_{K_2 \to \pi^+\pi^-\pi^0}$ is given in Eq. (3) and $g_{K_1 \to \pi^+\pi^-}$ is

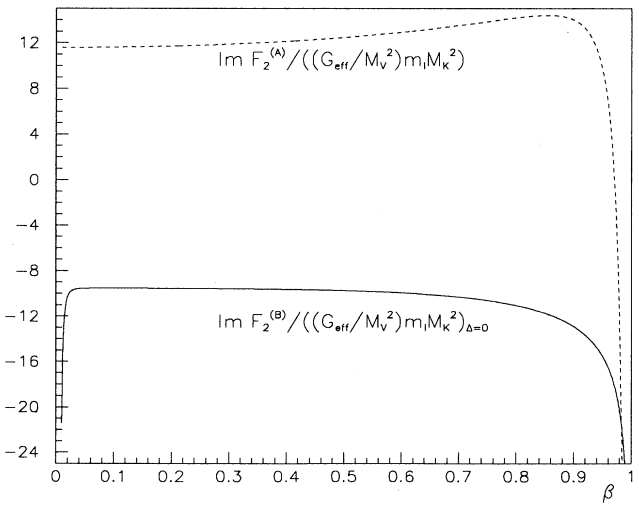

FIG. 14. Absorptive parts of the form factor $F_2(\beta)$ for $K_L \to \pi^0 l^+ l^-$ associated with VMD-type matrix element of $K_L \to \pi^0\gamma\gamma$.

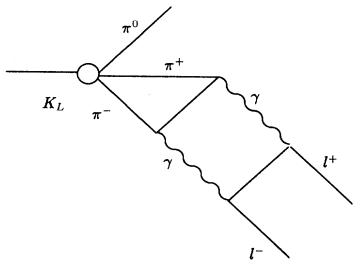

FIG. 15. Two-loop diagram for the *CP*-conserving 2γ contribution to $K_L \to \pi^0 l^+ l^-$.

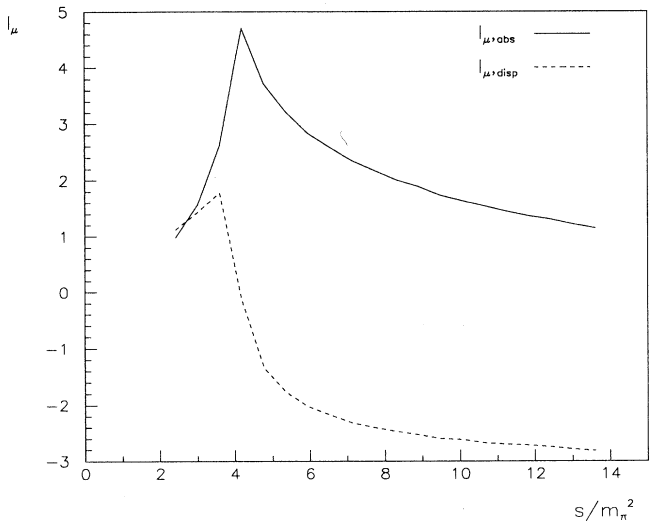

FIG. 16. Absorptive and dispersive contributions to $K_L \to \pi^0\mu^+\mu^-$ related to the pion-loop amplitude of $K_L \to \pi^0\gamma\gamma$ [relation between I and F_2^{loop} given in Eq. (34)].

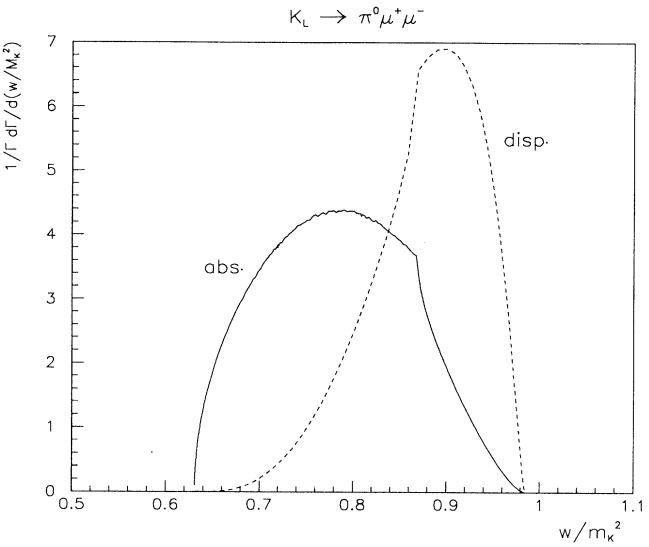

FIG. 17. Invariant mass spectrum of $\mu^+\mu^-$ pair in $K_L \to \pi^0\mu^+\mu^-$ (absorptive and dispersive parts of *CP*-conserving contribution).

determined by

$$\Gamma(K_1 \to \pi^+\pi^-) = \frac{|g_{K_1\to\pi^+\pi^-}|^2}{16\pi M_K}\left[1-\frac{4\mu^2}{M_K^2}\right]^{1/2} . \tag{35}$$

Figure 16 shows the s dependence of the functions $I_{\mu,\text{abs}}$ and $I_{\mu,\text{disp}}$ over the domain $4m_\mu^2 < s < M_K^2$. We have checked our numerical calculation with the values quoted in Ref. [19] for $s = M_K^2$, namely, $I_{\mu,\text{abs}}(s=M_K^2) = 1.21$ and $I_{\mu,\text{disp}}(s=M_K^2) = -2.82$. We have also verified that for $s < 4\mu^2$ (when only the 2γ intermediate state contributes to the absorptive part), the expression for $I_{l,\text{abs}}$ reduces to the well-known analytic result [20]

$$I_{l,\text{abs}} = \frac{\pi H(s)}{\beta}\ln\frac{1+\beta}{1-\beta} \quad (4m_l^2 < s < 4\mu^2) , \tag{36}$$

where

$$H(s) = -\frac{1}{2}\left[1-4\left\{\arcsin\left[\frac{1}{2}\left[\frac{1}{r_\pi^2}\right]^{1/2}\right]\right\}^2 \Big/ (1/r_\pi^2)\right] .$$

B. Decay spectrum and decay rate

Figure 17 shows the decay spectrum for the *CP*-conserving amplitude of $K_2 \to \pi^0\mu^+\mu^-$ as a function of w/M_K^2. We obtain, for the corresponding branching ratio (setting $G_{\text{eff}} = 0.15\times10^{-7}/M_K^2$),

$$B(K_2 \to \pi^0\mu^+\mu^-)|_{2\gamma} = 2.9\times10^{-12}(1+\rho_\mu) , \tag{37}$$

where

$$\rho_\mu = \frac{\Gamma_{\mu,\text{disp}}}{\Gamma_{\mu,\text{abs}}} \simeq 0.5 .$$

This result is interesting since it indicates that the *CP*-conserving branching ratio for $K_2 \to \pi^0\mu^+\mu^-$ is about the same size as the one for $K_2 \to \pi^0 e^+ e^-$. Pure phase space suggests [14]

$$B(K_2 \to \pi^0\mu^+\mu^-)/B(K_2 \to \pi^0 e^+ e^-) \approx 0.2 .$$

The enhancement of $K_2 \to \pi^0\mu^+\mu^-$ is connected with the existence of the F_2 form factor. Taking only the form factor F_1 into account, the result would be

$$B(K_2 \to \pi^0\mu^+\mu^-)_{2\gamma,F_1} = 3.9(1+1.8)\times10^{-14} .$$

Thus a μ:e ratio significantly greater than 0.2 would be a strong indication for the presence of a *CP*-conserving 2γ contribution in these decays.

V. *CP*-VIOLATING CONTRIBUTIONS TO $K_L \to \pi^0 l^+ l^-$

A. Direct *CP* violation

The short-distance interaction of quarks and leptons shown in Fig. 18 generates an effective Hamiltonian for $s \to d l^+ l^-$ of the form [21]

$$H_{\text{eff}} = \frac{G_F}{\sqrt{2}}\sum_{q=u,c,t} V_{qs}^* V_{qd}\{\tilde{C}_{V,q}Q_V + \tilde{C}_{A,q}Q_A\} , \tag{38}$$

where

$$Q_V = \frac{e^2}{4\pi}[\bar{s}\gamma_\mu(1-\gamma_5)d][\bar{e}\gamma^\mu e] ,$$

$$Q_A = \frac{e^2}{4\pi}[\bar{s}\gamma_\mu(1-\gamma_5)d][\bar{e}\gamma^\mu\gamma_5 e] .$$

This Hamiltonian gives rise to *CP*-violating contributions of the form $F_{V,A}^{\text{even}}$ in the $K_2 \to \pi^0 l^+ l^-$ amplitude, proportional to the *CP*-violating invariant

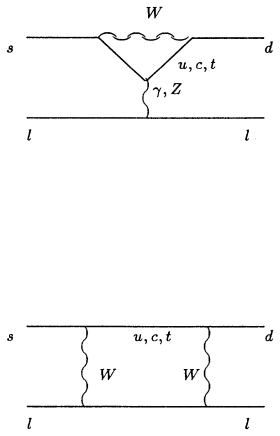

FIG. 18. Short-distance diagram for $s\bar{d} \to l\bar{l}$.

$\mathrm{Im}[V_{ts}^* V_{td}/V_{us}^* V_{ud}] = s_2 s_3 s_\delta$. The hadronic matrix element of the operator $\bar{s}\gamma_\mu(1-\gamma_5)d$, which occurs in Q_V and Q_A, may be related to the matrix element of the charged current operator $\bar{s}\gamma_\mu(1-\gamma_5)u$, which occurs in K_{l3} decay [we neglect contributions proportional to the $f_-(q^2)$, since $|f_-/f_+| \simeq 0.35 \pm 0.15$ [22], $f_-(q^2)$ and $f_+(q^2)$ being the conventional K_{l3} form factors]. The rate associated with direct *CP* violation is

$$B(K_2 \to \pi^0 e^+ e^-)|_{\mathrm{dir}} = 1 \times 10^{-5} (s_2 s_3 s_\delta)^2 [\tilde{C}_V^2 + \tilde{C}_A^2] , \tag{39}$$

where $\tilde{C}_{V,A}$ are functions of the top-quark mass with typical values $\tilde{C}_V = -0.5$, $\tilde{C}_A = 0.6$ for $m_t = 150$ GeV. With $s_2 s_3 s_\delta \simeq 0.5 \times 10^{-3}$, the direct contribution is 0.15×10^{-11}.

B. Indirect *CP* violation

Another source of *CP* violation is the small admixture of the *CP*-even K_1 state in the long-lived eigenstate

$$K_L = \frac{K_2 + \epsilon K_1}{(1+|\epsilon|^2)^{1/2}} . \tag{40}$$

Here *CP* is violated in the mass matrix, while the decay $K_1 \to \pi^0 l^+ l^-$ proceeds in a *CP*-conserving manner via a one-photon intermediate state. The contribution of this "indirect" *CP* violation can be parametrized as [21]

$$B(K_L \to \pi^0 e^+ e^-)|_{\mathrm{indir}} = B(K^+ \to \pi^+ e^+ e^-) \times \frac{\tau_{K_L}}{\tau_{K^+}} \frac{\Gamma(K_L \to \pi^0 e^+ e^-)|_{\mathrm{indir}}}{\Gamma(K_1 \to \pi^0 e^+ e^-)} r^2 , \tag{41}$$

where

$$|r| = \left[\frac{\Gamma(K_1 \to \pi^0 e^+ e^-)}{\Gamma(K^+ \to \pi^+ e^+ e^-)} \right]^{1/2} ,$$

The factor $|r|$ has the value 1 if the transition between the K and the π is $\Delta I = \frac{1}{2}$ as is the case for the short-distance amplitude which involves a transition from a strange to a down quark. However, in the presence of both $\Delta I = \frac{1}{2}$ and $\frac{3}{2}$ amplitudes, any value is possible. Model calculations have yielded values such as $|r| \approx 2.3$ [23], $|r| \approx 0.4$ [24], $|r| \approx 0.5$ [25], $|r| \approx 0.25$ or 2.5 [26], and $|r| \approx 4.6$ or 7.9 [27]. From Eq. (41) we calculate the branching ratio associated with indirect *CP* violation to be

$$B(K_L \to \pi^0 e^+ e^-)|_{\mathrm{indir}} = 0.58 \times 10^{-11} r^2 .$$

Taking into account the coherence of the "indirect" and "direct" amplitudes and their characteristic phases, the total *CP*-violating rate is [21]

$$B(K_L \to \pi^0 e^+ e^-)|_{\not CP} = \left\{ \left| 0.76 r e^{i\pi/4} + C_V \left[\frac{s_2 s_3 s_\delta}{10^{-3}} \right] i \right|^2 + \left[C_A \left[\frac{s_2 s_3 s_\delta}{10^{-3}} \right] \right]^2 \right\} \times 10^{-11} . \tag{42}$$

For $|r|$ equal to unity, this results in

$$B(K_L \to \pi^0 e^+ e^-)|_{\not CP} = \begin{cases} 0.46 \times 10^{-11} , & r = +1 , \\ 1.0 \times 10^{-11} , & r = -1 . \end{cases} \tag{43}$$

The corresponding branching ratios for the decays with muons in the final state are expected to be smaller by a factor 0.2 due to phase space.

C. *CP*-violating asymmetry and $l^+ l^-$ spectrum

Combining the *CP*-conserving and *CP*-violating amplitudes discussed in the previous sections, we can calculate the full decay spectrum $d\Gamma/dw\, d\Delta$ for $K_L \to \pi^0 l^+ l^-$ [see Eq. (25)]. Here we are particularly interested in the term linear in Δ, which gives rise to the *CP*-violating asymmetry between l^+ and l^-. The fact that the *CP*-conserving and *CP*-violating amplitudes are comparable and that the 2γ contribution to the former has a large absorptive part opens up the possibility of a sizable asymmetry between l^+ and l^-. We define [14]

$$\frac{d\Gamma(E_- > E_+)}{dw} = \int_0^{\Delta_0(s)} \frac{d\Gamma}{dw\, d\Delta} d\Delta , \qquad \frac{d\Gamma(E_- < E_+)}{dw} = \int_{-\Delta_0(s)}^{0} \frac{d\Gamma}{dw\, d\Delta} d\Delta , \tag{44}$$

which denote densities in the two halves of the Dalitz plot, defined by $E_- > E_+$ and $E_- < E_+$. A measure of *CP* violation is then given by the asymmetry

$$\mathcal{A}(w) = \frac{\frac{d\Gamma(E_- > E_+)}{dw} - \frac{d\Gamma(E_- < E_+)}{dw}}{\frac{d\Gamma(E_- > E_+)}{dw} + \frac{d\Gamma(E_- < E_+)}{dw}} . \tag{45}$$

The asymmetry depends, of course, on the ratio

$$r = \pm [\Gamma(K_1 \to \pi^0 e^+ e^-)/\Gamma(K^+ \to \pi^+ e^+ e^-)]^{1/2}$$

TABLE I. Summary of branching ratios and integrated l^+l^- asymmetries for $K_L \to \pi^0 e^+ e^-$ and $K_L \to \pi^0 \mu^+ \mu^-$ (input: $G_{\text{eff}} M_K^2 = 0.15 \times 10^{-7}$, $\rho_e = 1.5$, $\rho_\mu = 0.5$, $\tilde{C}_V = -0.5$, $\tilde{C}_A = 0.6$, $s_2 s_3 s_\delta = 0.5 \times 10^{-3}$).

		$K_L \to \pi^0 e^+ e^-$	$K_L \to \pi^0 \mu^+ \mu^-$
Branching ratio	*CP* conserving	4.1×10^{-12}	4.4×10^{-12}
	CP violating ($r = +1$)	4.6×10^{-12}	1.1×10^{-12}
	($r = -1$)	10.0×10^{-12}	2.3×10^{-12}
	($r = +\frac{1}{3}$)	1.3×10^{-12}	0.4×10^{-12}
	($r = -\frac{1}{3}$)	3.1×10^{-12}	0.9×10^{-12}
	($r = +3$)	45.4×10^{-12}	9.2×10^{-12}
	($r = -3$)	61.6×10^{-12}	13.1×10^{-12}
Asymmetry	$r = +1$	+16.0%	−8.3%
	$r = -1$	+16.9%	+11.2%
	$r = +\frac{1}{3}$	+23.6%	−1.5%
	$r = -\frac{1}{3}$	+23.0%	+5.8%
	$r = +3$	+2.5%	−15.0%
	$r = -3$	+6.2%	+14.3%

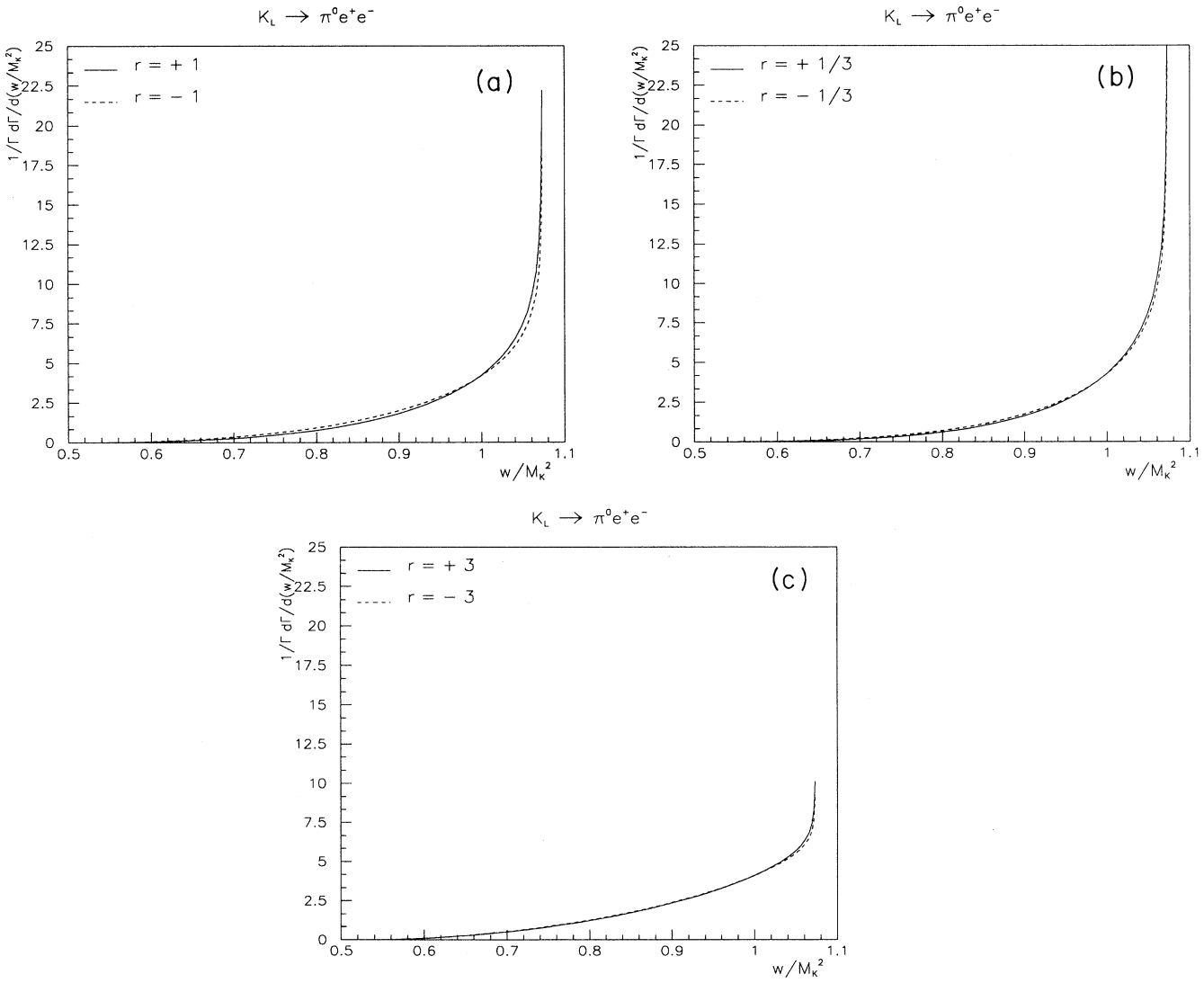

FIG. 19. Complete spectrum of e^+e^- pair in $K_L \to \pi^0 e^+ e^-$ for (a) $r = \pm 1$, (b) $r = \pm\frac{1}{3}$, and (c) $r = \pm 3$.

discussed in Sec. V B. We will use the values $\pm\frac{1}{3}$, ±1, and ±3, as illustrative of model-dependent calculations. Since the relative sign of the *CP*-conserving and *CP*-violating amplitudes is, *a priori*, not known, the asymmetry is calculable only up to an overall sign.

The result for the electron spectrum $d\Gamma/dw$ ($K_L \to \pi^0 e^+ e^-$), integrated over all Δ, is plotted in Figs. 19(a), 19(b), and 19(c) for $r=\pm1$, $\pm\frac{1}{3}$, and ±3, respectively. The spectrum is weighted toward large w, i.e., toward small invariant masses of the e^+e^- pair. For the case $r=\pm3$, the *CP*-violating rate dominates; the electron spectrum is flatter than for the cases $r=\pm\frac{1}{3}$ and $r=\pm1$, when *CP*-violating and *CP*-conserving rates are comparable. For the complete branching ratio, we obtain $B(K_L \to \pi^0 e^+ e^-)=\{(8.7,14.1),\ (5.4,7.2),\ (49.5,65.7)\}\times10^{-12}$ for $r=\{(+1,-1),(+\frac{1}{3},-\frac{1}{3}),(+3,-3)\}$.

The asymmetry is shown in Figs. 20(a), 20(c), and 20(d) for the cases $r=\pm1$, $\pm\frac{1}{3}$, and ±3, respectively. Figure 20(b) shows the asymmetry for the case of no direct *CP* violation, i.e., $s_\delta=0$. Thus this figure illustrates for the case $r=\pm1$ what happens in the so-called superweak model of *CP* violation. In all cases the asymmetry is sizable over the whole w domain. The effects are most striking when *CP*-violating and *CP*-conserving contributions are comparable, but reduced when one of them dominates, as can be seen in Fig. 20(d). We calculate integrated asymmetries of $\{(+16.0\%,+16.9\%),(+23.6\%,+23.0\%),\ (+2.5\%,+6.2\%)\}$ for the cases $\{(r=+1,r=-1),(r=+\frac{1}{3},r=-\frac{1}{3}),(r=+3,r=-3)\}$. For the case of the superweak model, the integrated

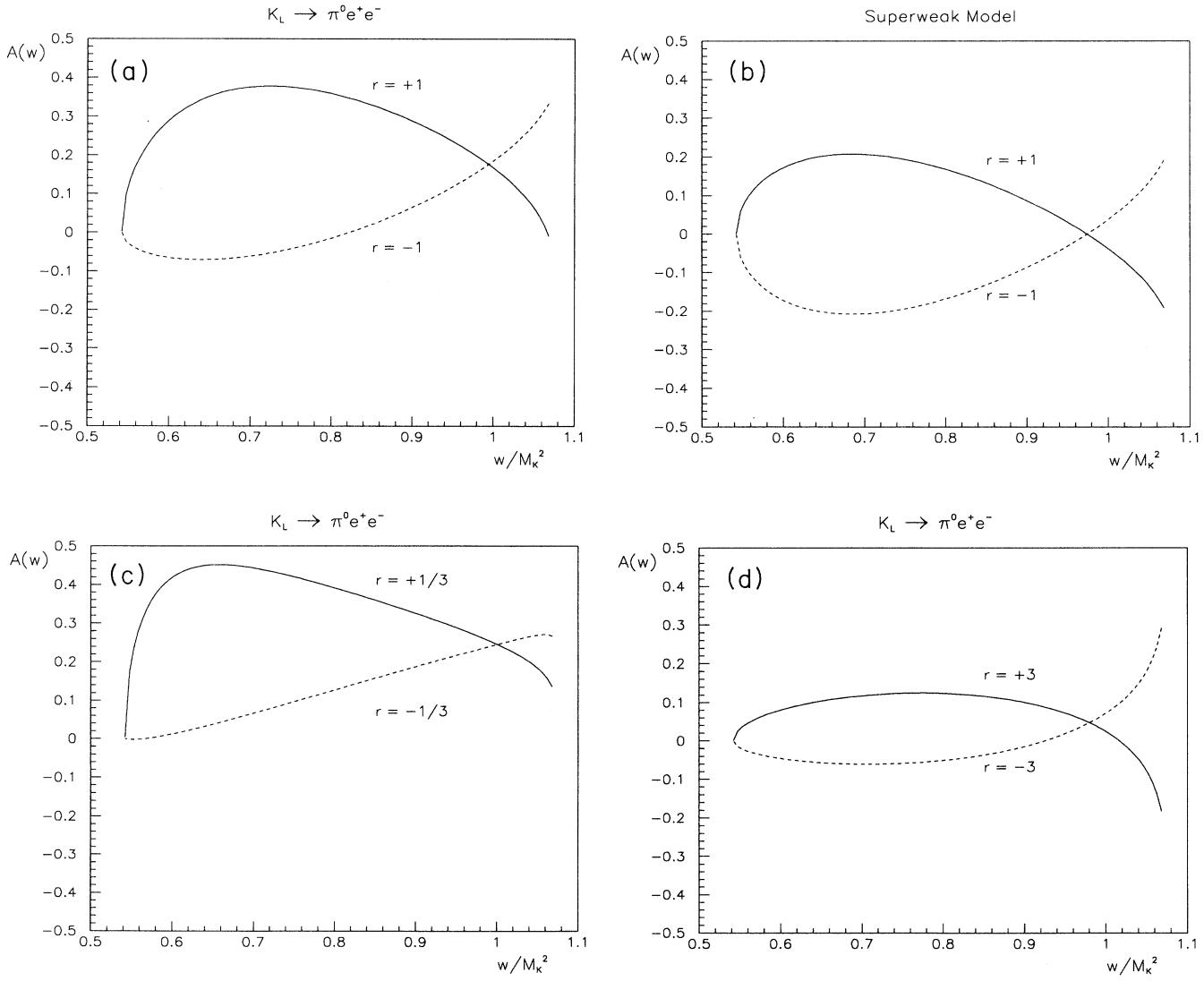

FIG. 20. *CP*-violating asymmetry between e^+ and e^- in $K_L \to \pi^0 e^+ e^-$ for (a) $r=\pm1$, (b) $r=\pm1$, superweak model, (c) $r=\pm\frac{1}{3}$, and (d) $r=\pm3$.

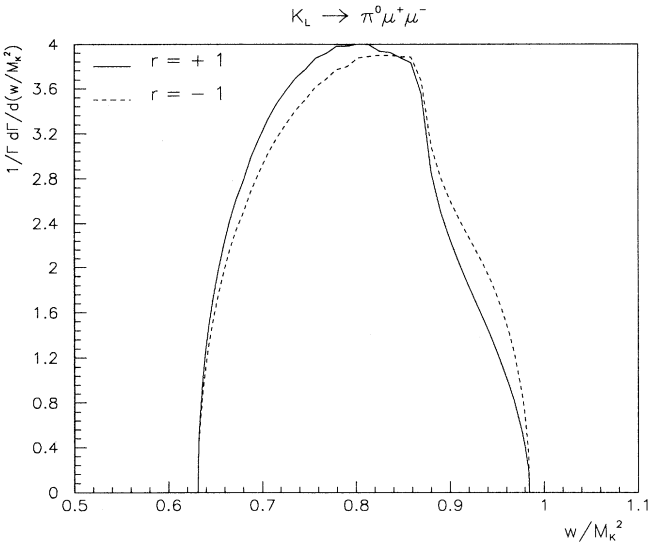

FIG. 21. Complete invariant mass spectrum of $\mu^+\mu^-$ pairs in $K_L\to\pi^0\mu^+\mu^-$ ($r=\pm1$).

asymmetry is $\{\mp3.2\%, \mp1.6\%, \mp2.5\%\}$ for $\{r=\pm1, r=\pm\frac{1}{3}, r=\pm3\}$. In principle, therefore, knowledge of the ratio r would permit one to test the existence of direct CP violation from a measurement of the e^+e^- asymmetry.

The muon spectrum $d\Gamma/dw(K_L\to\pi^0\mu^+\mu^-)$ is shown in Fig. 21 for the corresponding ratio $r=\pm1$. The spectrum is weighted toward the intermediate region of invariant masses of the $\mu^+\mu^-$ pair. The resulting asymmetries are shown in Figs. 22(a)–22(d). The integrated asymmetries are $\{(-8.3\%,+11.2\%), (-1.5\%,+5.8\%), (-15.0\%,+14.3\%)\}$ for the cases $\{(r=+1,r=-1), (r=+\frac{1}{3},r=-\frac{1}{3}), (r=+3,r=-3)\}$; for the superweak model, the integrated asymmetry is $\{\mp10.5\%, \mp4.0\%, \mp15.1\%\}$ for $\{r=\pm1,r=\pm\frac{1}{3},r=\pm3\}$. The branching ratio is $B(K_L\to\pi^0\mu^+\mu^-)=\{(5.5,6.7), (4.8,5.3), (13.6,17.5)\}\times10^{-12}$ for $r=\{(+1,-1), (+\frac{1}{3},-\frac{1}{3}), (+3,-3)\}$.

Our results for the branching ratios and asymmetries are summarized in Table I.

ACKNOWLEDGMENTS

We have benefited from discussions with Professor Lincoln Wolfenstein. One of us (P.H.) acknowledges the financial support of the Graduiertenförderungsgesetz Nordrhein-Westfalen.

APPENDIX

As noted in Sec. II D, the assumption that the vector-meson-mediated amplitude is determined by $K_2-\pi$, $K_2-\eta$, and $K_2-\eta'$ couplings leads to a value $|G|=0.2\times10^{-7}M_K^{-2}$. This determination involves, however, various assumptions such as nonet symmetry, $\eta-\eta'$ mixing, etc. We describe here a determination of the parameter G that avoids any reference to the detailed structure of the $K_2\rho\gamma$ and $K_2\omega\gamma$ vertices, but instead aims at obtaining a consistent picture of the experimentally measured decays $K_2\to\gamma\gamma$, the direct emission part of $K_2\to\pi^+\pi^-\gamma$ and $K_2\to\pi^0\gamma\gamma$ (see Fig. 5), based on the assumption that these decays are dominated by the same vertices. It is worth mentioning, as stated in [28] with respect to the direct emission amplitude of $K_L\to\pi^+\pi^-\gamma$, that "the data supports a modification to the standard $M1$ amplitude that includes a ρ propagator form factor."

Under the assumption of (ρ,ω) dominance, we have the following.

(i) The amplitude for $K_L\to\gamma\gamma$ is

$$A_1=\left[ea_\rho\frac{1}{M_K}\frac{1}{m_\rho^2}g_{\rho\gamma}+ea_\omega\frac{1}{M_K}\frac{1}{m_\omega^2}g_{\omega\gamma}\right]\times\epsilon^\mu\epsilon'^\nu k^\rho k'^\sigma\epsilon_{\mu\nu\rho\sigma}\ . \tag{A1}$$

(ii) The direct emission (magnetic dipole) amplitude of $K_L\to\pi^+\pi^-\gamma$ is

$$A_2=ea_\rho\frac{1}{M_K}\frac{1}{m_\rho^2}f_{\rho\pi\pi}\epsilon_{\mu\nu\rho\sigma}p_+^\mu p_-^\nu k^\rho\epsilon^\sigma\left[1-\frac{s}{m_\rho^2}\right]^{-1}. \tag{A2}$$

(iii) The vector-meson contribution to $K_L\to\pi^0\gamma\gamma$ is

$$M_K^2G=e(a_\omega+\tfrac{1}{3}a_\rho)M_Kf_{\omega\pi\gamma}\ . \tag{A3}$$

The decay rates are given by

$$\Gamma(K_L\to\gamma\gamma)=\frac{\alpha}{16}\left[\frac{g_{\rho\gamma}}{m_\rho^2}\right]^2M_K\left[a_\rho+\frac{1}{3}a_\omega\right]^2, \tag{A4}$$

$$\Gamma(K_L\to\pi^+\pi^-\gamma)_{\rm DE}=\frac{\alpha}{24\pi}a_\rho^2\frac{f_{\rho\pi\pi}^2}{4\pi}M_K\int_{\omega_{\min}}^{\omega_{\max}}d\omega\left[\frac{1}{M_K^2-2M_K\omega-m_\rho^2}\right]^2\times\omega^3\beta^3\left[1-\frac{2\omega}{M_K}\right], \tag{A5}$$

with

$$\beta=\left[1-\frac{4\mu^2}{M_K^2-2M_K\omega}\right]^{1/2},\quad \omega_{\max}=\frac{1}{2}M_K\left[1-\frac{4\mu^2}{M_K^2}\right].$$

Experimentally,

$$B(K_L\to\gamma\gamma)=(5.70\pm0.27)\times10^{-4}$$

(see Ref. [22]),

$$B(K_L \to \pi^+\pi^-\gamma)_{\rm DE} = (3.04 \pm 0.14) \times 10^{-5} \quad (E_\gamma > 20 \text{ MeV})$$

(see Ref. [28]). From these measured rates, we determine

$$|a_\rho| = 1.92 \times 10^{-7}, \quad |a_\rho + \tfrac{1}{3} a_\omega| = 1.04 \times 10^{-7},$$

which yield two solutions (up to an overall sign):

(i) $a_\rho = 1.92 \times 10^{-7}$, $a_\omega = -2.62 \times 10^{-7}$,

(ii) $a_\rho = 1.92 \times 10^{-7}$, $a_\omega = -8.89 \times 10^{-7}$.

(We discard the second solution since it gives an unacceptably high rate for $K_L \to \pi^0\gamma\gamma$.) Using the values in (i), we obtain the combination

$$|a_\omega + \tfrac{1}{3} a_\rho| = 1.98 \times 10^{-7}, \tag{A6}$$

which fixes the strength of the VMD contribution to $K_L \to \pi^0\gamma\gamma$:

$$G = e[a_\omega + \tfrac{1}{3} a_\rho] \frac{1}{M_K} f_{\omega\pi\gamma}. \tag{A7}$$

Using the value $f_{\omega\pi\gamma} = 7 \times 10^{-4}$ MeV^{-1}, we calculate $|G| M_K^2 = 0.21 \times 10^{-7}$. This estimate is not a calculation from first principles since it is possible to imagine numerous other contributions to the decay $K_L \to \pi^0\gamma\gamma$

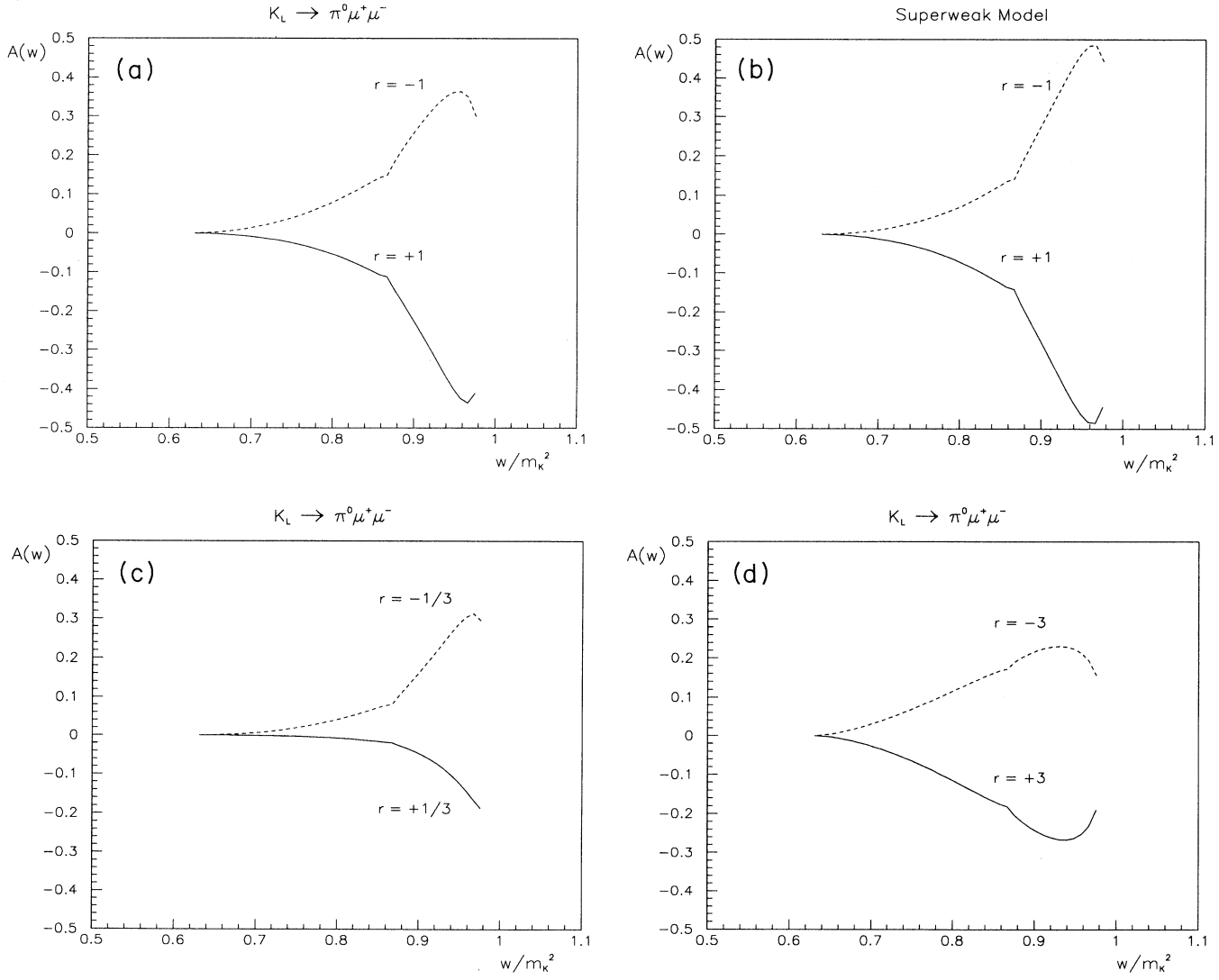

FIG. 22. *CP*-violating asymmetry between μ^+ and μ^- in $K_L \to \pi^0\mu^+\mu^-$ for (a) $r = \pm 1$, (b) $r = \pm 1$, superweak model, (c) $r = \pm\frac{1}{3}$, and (d) $r = \pm 3$.

(see, for example, [27]). However, the observation [28] of a ρ-propagator-like effect in the direct emission amplitude of $K_L \to \pi^+\pi^-\gamma$ and the measurement of the $K_L \to \gamma\gamma^*$ form factor [29], consistent with vector-meson-dominance behavior, support our assumption. We expect that our estimate of $|G| = 0.2 \pm 0.1$ covers some of the uncertainties of the model, e.g., possible further structure in the $K_2\rho\gamma$ and $K_2\omega\gamma$ vertices.

[1] NA31 Collaboration, G. D. Barr *et al.*, Phys. Lett. B **242**, 523 (1990).
[2] E731 Collaboration, V. Papadimitriou *et al.*, Phys. Rev. D **44**, 573 (1991).
[3] NA31 Collaboration, G. D. Barr *et al.*, Phys. Lett. B **284**, 440 (1992).
[4] L. M. Sehgal, Phys. Rev. D **41**, 161 (1990).
[5] L. M. Sehgal, Phys. Rev. D **6**, 367 (1972).
[6] G. Ecker, A. Pich, and E. de Rafael, Phys. Lett. B **189**, 363 (1987); Nucl. Phys. **B303**, 665 (1988); L. Capiello and G. Ambrosio, Nuovo Cimento A **99**, 153 (1988).
[7] T. Morozumi and H. Iwasaki, Prog. Theor. Phys. **82**, 371 (1989).
[8] T. Hambye, Int. J. Mod. Phys. A **7**, 135 (1992).
[9] L. M. Sehgal, in *Particles and Nuclei,* Proceedings of the XIIth International Conference on Particles and Nuclei, Cambridge, Massachusetts, 1990, edited by J. L. Matthews *et al.* [Nucl. Phys. **A527**, 721 (1991)].
[10] P. Ko and J. L. Rosner, Phys. Rev. D **40**, 3775 (1989).
[11] T. N. Truong, University of Chicago Report No. E.F.I. 89-57 (unpublished).
[12] G. Ecker, A. Pich, and E. de Rafael, Phys. Lett. B **273**, 481 (1990).
[13] J.Bijnens, S. Dawson, and G. Valencia, Phys. Rev. D **44**, 3555 (1991).
[14] L. M. Sehgal, Phys. Rev. D **38**, 808 (1988).
[15] J. Smith, Phys. Rev. **166**, 1629 (1968).
[16] J. Flynn and L. Randall, Phys. Lett. B **216**, 221 (1989).
[17] T. P. Cheng, Phys. Rev. **162**, 1734 (1967).
[18] H. B. Greenlee, Phys. Rev. D **42**, 3724 (1990).
[19] G. Ecker and A. Pich, Nucl. Phys. **B366**, 189 (1991).
[20] B. R. Martin, E. de Rafael, and J. Smith, Phys. Rev. D **2**, 179 (1970); **4**, 272(E) (1971).
[21] C. Dib, I. Dunietz, and F. J. Gilman, Phys. Rev. D **39**, 2639 (1989).
[22] Particle Data Group, K. Hikasa *et al.*, Phys. Rev. D **45**, S1 (1992).
[23] A. I. Vainshtein *et al.*, Yad. Fiz. **24**, 820 (1976) [Sov. J. Nucl. Phys. **24**, 427 (1976)].
[24] G. V. Efimov *et al.*, Z. Phys. C **52**, 129 (1991).
[25] C. Bruno and J. Prades, Z. Phys. C **57**, 585 (1993).
[26] G. Ecker, A. Pich, and E. de Rafael, Nucl. Phys. **B291**, 692 (1987); **B303**, 665 (1988).
[27] P. Ko, Phys. Rev. D **44**, 139 (1991).
[28] E731 Collaboration, E. Ramberg, Fermilab Report No. Fermilab-Conf-91/258, (unpublished).
[29] NA31 Collaboration, G. D. Barr *et al.*, Phys. Lett. B **240**, 283 (1990).